HHS Public Access

Author manuscript

Invest Radiol. Author manuscript; available in PMC 2018 April 01.

Published in final edited form as:

Invest Radiol. 2017 April ; 52(4): 198–205. doi:10.1097/RLI.0000000000000329.

Novel High Spatiotemporal Resolution Versus Standard-of-Care Dynamic Contrast-Enhanced Breast MRI: Comparison of Image Quality

Courtney K. Morrison, MS[1], **Leah C. Henze Bancroft, PhD**[1], **Wendy B. DeMartini, MD**[2], **James H. Holmes, PhD**[3], **Kang Wang, PhD**[3], **Ryan J. Bosca, PhD**[1], **Frank R. Korosec, PhD**[1,2], and **Roberta M. Strigel, MD, MS**[1,2]

[1]Department of Medical Physics, University of Wisconsin, 1111 Highland Avenue, Madison, Wisconsin 53705 USA

[2]Department of Radiology, University of Wisconsin School of Medicine and Public Health, 600 Highland Avenue, Madison, Wisconsin 53792 USA

[3]Global MR Applications and Workflow, GE Healthcare, 1111 Highland Avenue, Madison, Wisconsin 53705 USA

Abstract

Objective—Currently, dynamic contrast-enhanced breast MRI prioritizes spatial resolution over temporal resolution given the limitations of acquisition techniques. The purpose of our intra-patient study was to assess the ability of a novel high spatial and high temporal resolution DCE breast MRI method to maintain image quality compared to the clinical standard-of-care (SOC) MRI.

Materials and Methods—Thirty patients, each demonstrating a focal area of enhancement (29 benign, 1 cancer) on their SOC MRI consented to undergo a research DCE breast MRI on a second date. For the research DCE MRI, a method (DISCO) employing pseudo-random k-space sampling, view sharing reconstruction, two-point Dixon fat-water separation, and parallel imaging was used to produce images with an effective temporal resolution six times faster than the SOC MRI (27 seconds versus 168 seconds, respectively). Both the SOC and DISCO MR images were acquired with matching spatial resolutions of $0.8 \times 0.8 \times 1.6$ mm^3. Image quality (distortion/artifacts, resolution, fat suppression, lesion conspicuity, perceived SNR, and overall image quality) was scored by three radiologists in a blinded reader study.

Results—Differences in image quality scores between the DISCO and SOC images were all less than 0.8 on a 10-point scale, and both methods were assessed as providing diagnostic image quality in all cases. DISCO images with the same high spatial resolution, but six times the effective temporal resolution as the SOC MR images were produced, yielding 20 post-contrast time-points with DISCO compared with three for the SOC MRI, over the same total time interval.

Corresponding Author Information: Roberta M. Strigel, MD, MS, Address: 600 Highland Avenue, Madison, WI 53792-3252, Phone: (608) 265-0805, Fax: (608) 265-3134, rstrigel@uwhealth.org.

Conclusions—DISCO provided comparable image quality compared to the SOC MRI, while also providing six-times faster effective temporal resolution and the same high spatial resolution.

Keywords

Breast Cancer; Accelerated MRI; Fat-water Separation

Introduction

Breast MRI is currently the most sensitive imaging test for identifying breast cancer, capable of detecting malignancy that is occult to physical exam and other imaging modalities (1-3). This has led to a rapid increase in the use of breast MRI (4-7), particularly in those patients at high risk for the development of breast cancer (8, 9). A typical breast MRI protocol includes multiple imaging sequences, the most important of which is a high spatial resolution T_1-weighted dynamic contrast-enhanced sequence. DCE breast MRI derives its sensitivity by demonstrating the enhancement of lesions following the intravenous injection of gadolinium-chelated contrast agents, revealing findings that are predictive of, but not definitive for, malignancy. It is used to detect lesions and to characterize lesion morphology and signal enhancement over time (kinetics) based on the American College of Radiology Breast Imaging Reporting and Data System (BI-RADS) Atlas (10), which defines standard lesion types, morphologic features, and kinetics.

Ideally, DCE breast MRI would provide both high spatial resolution to characterize lesion morphology and high temporal resolution to characterize lesion kinetics to improve diagnostic accuracy (1, 11-17). However, conventional methods of MRI data acquisition have precluded obtaining images with the necessary high spatial resolution and simultaneous high temporal resolution (1, 15, 18); currently high spatial resolution is prioritized clinically (1, 15, 18). In addition to the spatial and temporal resolution demands, DCE breast MRI must also balance sufficient signal-to-noise ratio (SNR), an adequately large field-of-view (FOV) to include both breasts, and homogeneous fat suppression. Many of these requirements pose directly competing demands. For example, high spatial resolution and active fat suppression both require long scan times and lead to reduced temporal resolution. Nonetheless, suppression or removal of the fat signal is essential for improving the conspicuity of lesions since the signal from fat can appear iso-intense to contrast-enhanced breast lesions. Fat suppression can be achieved in various ways, including fat-selective inversion or saturation pulses, water-only excitation pulses, or fat-water separation techniques such as Dixon methods (19), all of which have different temporal costs. Another fat suppression method, which does not require additional acquisition time, is subtraction, but it is prone to signal intensity errors due to motion.

Many recent technical advancements in MRI have focused on accelerating data acquisition. Some of these advancements, such as parallel imaging (20-22), are widely accepted and used in clinical breast MRI; however, other data acquisition acceleration techniques, such as undersampled radial imaging (23, 24) and k-t segmentation schemes (25, 26), are less well-established. The more randomized k-t sampling approaches that have been introduced in recent years were proposed to help reduce temporal blurring and coherent artifacts (26, 27)

as compared with earlier methods that did not use random sampling and updated discrete, non-intermingled k-space regions. Several of these acceleration techniques rely on view sharing to reconstruct an image volume by combining high spatial frequency k-space data from adjacent undersampled k-space intervals. These methods may better characterize breast lesion kinetics while preserving the high spatial resolution required clinically (26, 28, 29).

While rapid updates of the central k-space region in view sharing create a realistic impression of dynamic contrast passage, particularly in large, homogeneous structures, which are predominantly represented by the low spatial frequency content at the center of k-space, less frequent updates of the k-space periphery could potentially degrade the image quality and/or fail to capture rapid signal changes (30, 31). In particular, the high spatial frequency regions of k-space heavily influence the appearance of edges and small structures in the image. Thus, updating these regions of k-space less frequently could potentially lead to inaccurate depiction of the signal enhancement of anatomic detail, including lesion edges, which could impact characterization of lesion morphologic features. If the depiction of fine anatomic detail is compromised by view sharing, then the drawbacks of these novel techniques may outweigh the potential benefits offered by improved demonstration of kinetics.

In this study, we performed high spatiotemporal resolution DCE breast MRI using the DIfferential Subsampling with Cartesian Ordering (DISCO) (26, 29) sampling pattern in combination with view sharing, two-point Dixon fat-water separation, and parallel imaging. This method provides improved temporal resolution while maintaining the high spatial resolution used in the clinical setting. Use of the DISCO sampling pattern has previously been demonstrated for breast imaging using high temporal resolution but without maintaining the clinically-required high spatial resolution (29). In the intra-patient study described here, we assessed whether DISCO demonstrates equivalent image quality to the current clinical standard-of-care (SOC) DCE breast MRI method when implemented with the same high spatial resolution but higher temporal resolution.

Materials and Methods

Patients

Thirty patients demonstrating a focal area of enhancement on their clinical MRI exams performed between 9/2013 and 5/2014 provided informed consent to participate in this IRB-approved, HIPAA-compliant intra-individual study. On a return visit, patients underwent a research DCE breast MRI described in greater detail below. Exclusion criteria included any intervention, such as biopsy, surgery, or chemotherapy, between the clinical and research exams.

For reporting purposes, patient age, clinical indication for the MRI, and benign versus malignant outcome for the focal area of enhancement were obtained from review of the patient images and medical record (Epic Systems Corporation, Verona, WI; McKesson PACS, Newton, MA). The clinical outcome of the focal area of enhancement was based on biopsy results, imaging features, and/or clinical/imaging follow-up.

MRI data acquisition

Clinical standard-of-care breast MRI ("SOC")—The SOC MRI was performed on a 1.5 T scanner (Signa HDxt, GE Healthcare, Waukesha, WI) with an 8-channel breast coil (Sentinelle, Invivo, Gainesville, FL). Immobilization paddles were used to stabilize the breasts to reduce motion. Images were acquired in the axial plane using a DCE T_1-weighted 3D fast spoiled gradient echo (FSPGR) sequence with intermittent chemical fat saturation (VIBRANT, GE Healthcare) and a parallel imaging factor of two in the k_z (slice) direction using the vendor-provided coil sensitivity-based ASSET option. Images with a temporal resolution of 168 s were obtained with one fully-sampled image time frame acquired before and three fully-sampled image time frames acquired after the administration of a gadolinium-based contrast agent. Rectilinear Cartesian k-space sampling was used, and the center of k-space was acquired midway through the acquisition. Thus, the center of k-space for the first post-contrast image time frame was acquired approximately 84 s after the start of injection of the contrast agent. The imaging matrix was 384 × 384 with a FOV of 32 cm × 32 cm and an in-plane spatial resolution of 0.8 mm × 0.8 mm. The acquired slice thickness was 1.6 mm, and a factor of two zero filling was used in the slice-encoding dimension. Remaining sequence parameters are given in Table 1.

Research high spatiotemporal resolution MRI ("DISCO")—DISCO MRI was performed on a 1.5 T scanner (Optima MR 450w, GE Healthcare) with an 8-channel breast coil (GE Healthcare). The patient positioning was the same as that used in the SOC exam with immobilization paddles used to stabilize each breast. Images were acquired in the axial plane. High spatiotemporal resolution T_1-weighted DCE MRI was performed using a variable density, pseudo-random k-space sampling pattern (26), as shown in Figure 1, in combination with two-point Dixon fat-water separation, view sharing reconstruction, and the vendor-provided coil-by-coil data-driven parallel imaging method (ARC, GE Healthcare). The DISCO sequence used in this study was a prototype version of a sequence that has since been made commercially available.

The k-space sampling pattern was such that k_y-k_z-space was segmented into two regions. The central region "A", which consisted of 16% of the k-space views, was fully sampled, less any parallel imaging undersampling. The center of the A region also included the auto-calibration lines used for parallel imaging. The outer region "B" was undersampled by a factor of three in addition to the parallel imaging undersampling, resulting in sub-regions B_1, B_2, and B_3. The full A region along with a single B sub-region was sampled in every k-space interval. Center out sampling was used. The sampling pattern was incorporated into a 3D FSPGR dual-echo sequence with bipolar readout gradients. The two echoes were acquired when fat and water were in-phase and opposed-phase to allow for two-point Dixon fat-water separation. The images for each time frame were reconstructed with data from the A region and B sub-region acquired within that k-space interval as well as the B sub-region data from the two preceding k-space intervals (backward view sharing) (Figure 1). Following backward view sharing reconstruction, fat-only and water-only images were generated using a two-point Dixon method with improved phase correction (32).

In this work, the time required to collect all the data used for reconstruction of a single, fully-sampled image time frame, including the data shared from other neighboring k-space intervals, will be referred to as the "temporal footprint," and the time between the acquisitions of the central region of k-space will be referred to as the "effective temporal resolution" (Figure 1). The k-space sampling pattern and view sharing reconstruction used in DISCO allows for a higher effective temporal resolution than is achievable with fully-sampled techniques because only one-third of the B region is acquired in each k-space interval. However, the view sharing reconstruction introduces a longer temporal footprint because views from preceding k-space intervals are used to reconstruct each successive image time frame. With the view sharing approach used here, data from three k-space intervals were used to reconstruct a single, fully-sampled image time frame (Figure 1).

In this study, one pre- and 20 post-contrast image time frames were produced with an effective temporal resolution of 27 s and a temporal footprint of 71 s (Figure 1). The imaging matrix was 412 × 412 with a 34 cm × 34 cm FOV and an in-plane spatial resolution of 0.8 mm × 0.8 mm. The slice thickness was 1.6 mm and a factor of two zero filling was used in the slice-encoding direction. Remaining sequence parameters are given in Table 1.

Contrast agent—A weight-based dose (0.1 mmol/kg) of a gadolinium-based contrast agent (gadobenate dimeglumine, Multihance, Bracco Inc., Milan, Italy) was administered intravenously followed by the administration of a 20 mL saline flush, both injected at a rate of 2 mL/s using a power injector, for both DISCO and the SOC MRI exams.

Image quality assessment

The DISCO and SOC images were independently scored for image quality by three fellowship-trained radiologists specializing in breast imaging with two, three, and 11 years of experience, respectively. Readers reviewed all slices from a single post-contrast time frame from both the DISCO and SOC DCE exams for each patient. For the SOC MRI, the readers reviewed all slices from the first post-contrast time frame corresponding to the acquisition of the center of k-space at ~84 s after the start of the injection. For DISCO, the readers reviewed all slices of the water images from the fifth post-contrast time frame corresponding to the acquisition of the center of k-space at ~108 s after the start of the injection. This time frame was chosen based on a prior qualitative evaluation where a fellowship-trained radiologist specializing in breast imaging with seven years of experience determined which time frame demonstrated the highest lesion-to-parenchyma contrast. On average, the fifth time frame was determined to represent the highest lesion-to-parenchyma contrast, and thus this time frame was used for the formal reader studies. Readers did not review the DISCO fat images. The order of the methods and the order of the patients were randomized within each reading session. Each reader reviewed the images from both methods, one method at a time. A focal area of enhancement to be assessed for lesion conspicuity was pre-selected by a fellowship-trained radiologist specializing in breast radiology with seven years of experience and indicated on the post-contrast time frame for each method with an arrow. Images were scored on a scale ranging from one (worst) to 10 (best) in the following categories: image distortion/artifacts, resolution/detail, quality/uniformity of fat suppression, lesion conspicuity, perceived SNR, and overall image quality.

Readers also assessed images for diagnostic image quality (“yes” or “no”). Readers were able to review all slices from the chosen post-contrast time frame for all components of the image quality assessment, and all components of the image quality assessment were performed in a single session per reader. Each reader was blinded to the results of the other readers.

Statistical analysis

Statistical analysis of the pooled results from the three readers was performed with a generalized estimating equation (GEE) model accounting for sequence (independence working correlation matrix with a robust sandwich covariance estimate); potential reader or reader-by-sequence interaction terms were not explicitly modeled. $P < 0.05$ (two-sided) was the criterion for statistical significance and R 3.1.0 (R Core Team 2014) was used for all statistical analyses (R Foundation for Statistical Computing, Vienna, Austria).

Results

Thirty women with an average age of 45 (range 28 to 65) years underwent both the DISCO and SOC exams. Clinical indications for the breast MRI exams were high risk screening in 24/30 (80%) and diagnostic in 6/30 (20%); diagnostic indications included four short-term interval follow-up studies, one problem solving, and one staging/extent of disease in a patient with a new diagnosis of breast cancer. The focal areas of enhancement selected in this study included seven biopsy-proven benign findings (four fibroadenomas, one fat necrosis, one apocrine metaplasia, one fibrocystic changes), five benign intramammary lymph nodes, five masses that were benign based on ≥ two years of follow-up, one malignancy (ductal carcinoma in situ), and 12 focal areas of benign background parenchymal enhancement.

Based on results from the reader study, image quality was determined to be similar between DISCO and the SOC method. Mean differences in all categories of image quality between DISCO the SOC method were never greater than 0.8 on the 10-point scale (Table 2). DISCO performed better for quality/uniformity of fat suppression (8.8 vs. 8.0, $P < 0.01$). The improved fat suppression of DISCO is shown in a patient example in Figure 2. The SOC method performed better for resolution/detail (8.2 vs. 7.9; $P < 0.01$), lesion conspicuity (8.0 vs. 7.5, $P = 0.02$), perceived SNR (8.2 vs. 7.4; $P < 0.01$), and overall image quality (8.1 vs. 7.7; $P < 0.01$). Both DISCO and the SOC method were scored as providing adequate diagnostic image quality in all 30 cases. A representative patient case demonstrating the similar image quality is shown in Figure 3.

Figure 4 shows a boxplot of the mean reader scores per patient from all three readers for all image quality categories. Image distortion/artifacts, resolution/detail, quality/uniformity of fat suppression, perceived SNR, and overall image quality were scored as 6 or higher for all cases for both DISCO and the SOC method. In regards to lesion conspicuity, three cases were scored less than 6 on DISCO while the SOC images were scored above 6 (3.7 vs. 8.3, 5.3 vs. 8.0, and 5.7 vs. 7.0). Conversely, the lesion conspicuity was scored as 5.3 on the SOC images for one case while DISCO was scored as 6.7. Examples of the range of lesion conspicuity scores are shown in Figure 5.

DISCO provided 17 additional time frames, with six-fold higher effective temporal resolution, improving the characterization of the signal intensity-time curve compared with the SOC method, as shown in Figure 6. In the example in Figure 6, DISCO provided additional time points and demonstrated higher peak enhancement than the lower temporal resolution SOC method in part because the signal was not averaged across the longer acquisition time of a single time frame in DISCO as it was in the SOC method.

Discussion

In this intra-patient study of 30 patients, we evaluated a novel MRI method implemented in a clinically-relevant manner that did not compromise the high spatial resolution used with the SOC method currently performed at our institution (0.8 × 0.8 × 1.6 mm at 1.5 T) and with an effective temporal resolution of 27 s, which is six-times faster than the temporal resolution of the SOC method (168 s). This novel technique uniquely undersamples k-space and employs view sharing image reconstruction, two-point Dixon fat-water separation, and parallel imaging to provide fat-suppressed DCE breast MR images. Assessed differences in image quality between DISCO and the SOC method were 0.8 or less on a 10-point scale and adequate diagnostic image quality was maintained for all cases.

An advantage of DISCO is the improved fat suppression provided by the two-point Dixon technique. This is important in breast MRI where the unsuppressed signal from fat can appear iso-intense to enhancing breast lesions and confound morphologic assessment. Uniform suppression of fat signal is particularly challenging in breast MRI due to B_0 field inhomogeneity given the air-tissue interface surrounding each breast and variations in tissue types within the breast. Dixon methods have been previously demonstrated to improve the robustness of fat-water separation in the presence of B_0 inhomogeneities and can be advantageous in the challenging breast MRI environment (33). Fat-water separation techniques such as the one employed here are less sensitive to B_0 inhomogeneities than other fat suppression techniques including the intermittent fat saturation pulse used in the SOC method, especially at higher field strength (32). Even at 1.5 T where B_0 inhomogeneities are less of a concern, DISCO demonstrated improved fat suppression relative to the SOC method. While this fat suppression technique is not unique to DISCO, two-point Dixon adversely affects temporal resolution due to the acquisition of two echoes. Since the DISCO sampling pattern undersamples k-space in each k-space interval and uses view sharing to produce fully-sampled images, DISCO achieves a time savings such that two echoes can be acquired while still improving the effective temporal resolution compared to the temporal resolution of the fully-sampled SOC method.

Several accelerated MRI methods, including DISCO, use view sharing reconstructions, in which the low spatial frequency regions of k-space are updated very frequently but the high spatial frequency regions of k-space are updated less frequently. We found that the image quality was comparable between DISCO and the SOC method; thus, our results support the use of view sharing with this sampling approach to improve the effective temporal resolution while maintaining high spatial resolution. In addition, the subset of low spatial frequency and undersampled high spatial frequency k-space data collected within a given k-space

interval for DISCO is too heavily undersampled to produce a diagnostic image. Thus, the inclusion of view-shared data improves image quality and lesion depiction.

In this study, we demonstrated that DISCO offers the ability to acquire additional time frames during contrast agent uptake and washout, enabling more detailed characterization of lesion signal intensity-time curves while preserving image quality. This more detailed characterization of signal intensity-time curves is important since previous work has shown that the shape of the signal intensity-time curve is predictive of malignancy and thus is used in routine clinical practice to improve both sensitivity and specificity for breast cancer (10, 11). For example, malignancies most characteristically exhibit fast enhancement after contrast injection and washout in the delayed phase after peak signal intensity is reached (10). For the image quality assessment, readers reviewed a single early post-contrast time frame from each method. Given the temporal resolution of the SOC method, only one time frame, with the center of k-space acquired at ~84 s post-contrast, was within the window for an early phase post-contrast series, and so the first SOC time frame was used in the reader study. A preliminary qualitative evaluation of the DISCO time frames demonstrated that the fifth post-contrast time frame, with the center of k-space acquired at ~108 s post-contrast, exhibited the highest lesion-to-parenchyma contrast and, for this reason, was used in the reader study. The reason why the DISCO time frame that exhibited the highest lesion-to-parenchyma contrast was delayed compared to the SOC time frame is unclear. However, DISCO provides higher effective temporal resolution than the SOC method and therefore should be able to more accurately identify the time of peak lesion-to-parenchyma contrast. The time of peak contrast on the SOC images could have occurred at any time during the long acquisition of the first post-contrast time frame, meaning anywhere between zero to 168 s post-contrast.

Additionally, the reason why the reader scores for lesion conspicuity were slightly lower for DISCO compared with the SOC method is also unclear. One possible explanation is the backward view sharing used to reconstruct the DISCO images. However, the signal contrast of an image is dominated by the low spatial frequency k-space data, which were collected in every k-space interval of the DISCO acquisition. Thus, the backward view sharing method likely did not affect the overall signal contrast of the DISCO images. However, sharing high spatial frequency data from previous k-space intervals, especially from k-space intervals in which data were acquired prior to the arrival of contrast agent, might possibly affect the depiction of edges and fine detail and may have contributed to the lower lesion conspicuity scores of DISCO. Nonetheless, the DISCO and SOC images from all patients were still determined to have diagnostic image quality. Additional study is needed to more fully understand the effects of view sharing on the depiction of lesions.

To overcome the compromise between spatial and temporal resolution, several techniques have recently been applied to DCE breast MRI. Saranathan et al. demonstrated a different implementation of the DISCO sampling pattern in breast MRI at 3.0 T (29). In that study, the DISCO sampling pattern was combined with the keyhole approach (34) to improve the spatial resolution of their sequence ($1.1 \times 1.1 \times 1.2$ mm^3) and reduce spatial blurring compared to fully-sampled VIBRANT-FLEX images ($1.1 \times 2.5 \times 4$ mm^3). In contrast, we

used a clinically-acceptable high spatial resolution for all time frames simultaneously with improved temporal resolution.

Another method, TWIST, utilizes a k-space sampling pattern similar to DISCO and also employs view sharing reconstruction; however, with TWIST, the k-space sampling trajectory spirals in and then spirals back out within each k-space interval, which is different from the k-space sampling trajectory used in DISCO, which only spirals out within each k-space interval. The use of TWIST has been demonstrated in breast MRI, but most published studies have relied on subtraction for fat suppression (25, 35). Le et al. investigated the application of TWIST with Dixon fat suppression and, similar to our results, found that the Dixon method provided improved fat suppression relative to the conventional method (28). Tudorica et al. provided further vaildation of TWIST in the breast by assessing morphologic characterization of lesions in 31 patients who were scanned with TWIST using water excitation for fat suppression and found that the characterization of lesion morphology was preserved (36). In both these studies, late-phase post-contrast images from TWIST and a conventional gradient echo acquisition were compared. Our result of similar image quality between the high spatiotemporal DISCO method and the SOC method is similar to findings from these investigators; however, we used a study design that allowed us to make intra-individual comparisons of the more clinically-relevant early-phase post-contrast images and acquired additional time-points for improved characterization of the entire signal intensity-time curve.

Although this study demonstrated a six-fold improvement in the effective temporal resolution relative to the SOC at our institution, producing images with higher effective temporal resolution than those demonstrated here can likely be achieved at higher field strength by employing increased parallel imaging factors, which may be enhanced by improved radiofrequency coil design, and with the addition of advanced reconstruction techniques such as compressed sensing. These advancements may allow for sufficiently high temporal resolution to estimate quantitative parameters from pharmacokinetic modeling of gadolinium contrast agents that could prove useful in clinical and research settings in order to improve diagnostic accuracy, monitor response to breast cancer therapy, and predict patient survival (37-40). Furthermore, this technique would be amenable to an abbreviated screening protocol such the one proposed by Kuhl et al. (41) by providing multiple early post-contrast time frames that can be evaluated to detect and asses lesions. This additional information is gained without a loss to the spatial resolution or image quality.

The use of a two-point Dixon technique, such as the one used in this study, allows for reconstruction of fat-only images in addition to the water-only images. Images showing fat are commonly acquired separately using a T_1-weighted FSPGR sequence without fat suppression as part of a complete clinical breast MRI protocol to assist the radiologist with assessing anatomy and lesion differential diagnosis. Availability of the fat-only DISCO images obviates the need for the separate acquisition of the non-fat suppressed T_1-weighted sequence and reduces exam time, thereby improving workflow and patient comfort. Furthermore, a two-point Dixon method, such as the one used with DISCO, could prove beneficial in the realm of quantitative imaging; recent work has shown that a two-point

Dixon method reduces bias in quantitative pharmacokinetic modeling of DCE MRI in the presence of fat (42, 43).

Though the results of this study are promising, there were some limitations. A 1.5 T scanner and 8-channel coil were used for all exams but the exact scanner-coil combination differed between DISCO and the SOC method due to scanner and coil availability at our institution; however, we do not believe that these differences had a significant impact on image quality. Similarly, the parallel imaging methods and factors differed between DISCO and the SOC method. Although we do not believe that the difference in parallel imaging methods (data-driven for DISCO and coil sensitivity-based for the SOC method) had a significant effect on image quality, the increased parallel imaging factors used with DISCO, combined with other factors such as the higher receiver bandwidth, may have contributed to the difference in perceived SNR between DISCO and the SOC method noted in the image quality assessment.

In conclusion, this study provides initial results obtained using a new high spatiotemporal resolution technique for DCE breast MRI in a clinical environment using an intra-individual study design. We successfully performed high spatiotemporal resolution breast MRI with DISCO matching the high spatial resolution of SOC DCE breast MRI while improving the temporal resolution six-fold. DISCO provided improved fat suppression relative to the SOC method, and diagnostic image quality was maintained in all cases.

Acknowledgments

We appreciate support from the University of Wisconsin Departments of Radiology and Medical Physics, Radiological Society of North America Research & Education Foundation, and GE Healthcare. Research reported in this publication was also supported by the National Cancer Institute of the National Institutes of Health under Award Number T32CA009206. The content is solely the responsibility of the authors and does not necessarily represent the official views of the National Institutes of Health.

References

1. Kuhl CK. Current status of breast MR imaging: Part 1. Choice of technique, image interpretation, diagnostic accuracy, and transfer to clinical practice. Radiology. 2007; 244(2):356–78. [PubMed: 17641361]
2. Lehman C, Isaacs C, Schnall MD, et al. Cancer yield of mammography, MR, and US in high-risk women: Prospective multi-institution breast cancer screening study. Radiology. 2007; 244(2):381–8. [PubMed: 17641362]
3. DeMartini WB, Lehman C. Review of current evidence-based clinical applications for breast magnetic resonance imaging. Top Magn Reson Imaging. 2008; 19(3):143–50. [PubMed: 18941394]
4. DeMartini WB, Ichikawa L, Yankaskas BC, et al. Breast MRI in community practice: equipment and imaging techniques at facilities in the Breast Cancer Surveillance Consortium. J Am Coll Radiol. 2010; 7(11):878–84. [PubMed: 21040870]
5. Elmore L, Margenthaler JA. Use of breast MRI surveillance in women at high risk for breast cancer: a single-institutional experience. Ann Surg Oncol. 2010; 17(Suppl 3):263–7.
6. Stout NK, Nekhlyudov L. Early uptake of breast magnetic resonance imaging in a community-based medical practice, 2000-2004. J Womens Health (Larchmt). 2011; 20(4):631–4. [PubMed: 21413899]
7. Wernli KJ, DeMartini WB, Ichikawa L, et al. Patterns of breast magnetic resonance imaging use in community practice. JAMA Intern Med. 2014; 174(1):125–32. [PubMed: 24247555]
8. Saslow D, Boetes C, Burke W, et al. American Cancer Society guidelines for breast screening with MRI as an adjunct to mammography. CA Cancer J Clin. 2007; 57(2):75–89. [PubMed: 17392385]

9. Sardanelli F, Podo F, Santoro F, et al. Multicenter surveillance of women at high genetic breast cancer risk using mammography, ultrasonography, and contrast-enhanced magnetic resonance imaging (the high breast cancer risk italian 1 study): final results. Invest Radiol. 2011; 46(2):94–105. [PubMed: 21139507]
10. Morris, EA., Comstock, CE., Lee, CH., et al. ACR BI-RADS Atlas, Breast Imaging Reporting and Data System. Reston, VA: American College of Radiology; 2013. ACR BI-RADS Magnetic Resonance Imaging.
11. Kuhl CK, Mielcareck P, Klaschik S, et al. Dynamic breast MR imaging: Are singal intensity time course data useful for differential diagnosis of enhancing lesions? Radiology. 1999; 211(1):101–10. [PubMed: 10189459]
12. Kuhl CK, Schild HH. Dynanic image interpretation of MRI of the breast. J Magn Reson Imaging. 2000; 19:965–74.
13. Bluemke D, Gatsonis C, Chen M, et al. Magnetic resonance imaging of the breast prior to biopsy. JAMA. 2004; 292(22):2735–42. [PubMed: 15585733]
14. Vomweg TW, Teifke A, Kunz RP, et al. Combination of low and high resolution sequences in two orientations for dynamic contrast-enhanced MRI of the breast: more than a compromise. Eur Radiol. 2004; 14(10):1732–42. [PubMed: 15378253]
15. Kuhl CK, Schild HH, Morakkabati N. Dynamic bilateral contrast-enhanced MR imaging of the breast: Tradoff between spatial and temporal resolution. Radiology. 2005; 236(3):789–800. [PubMed: 16118161]
16. Schnall MD, Blume J, Bluemke DA, et al. Diagnostic architectural and dynamic features at breast MR imaging: Multicenter study. Radiology. 2006; 238(1):42–53. [PubMed: 16373758]
17. Veltman J, Stoutjesdijk M, Mann R, et al. Contrast-enhanced magnetic resonance imaging of the breast: the value of pharmacokinetic parameters derived from fast dynamic imaging during initial enhancement in classifying lesions. Eur Radiol. 2008; 18(6):1123–33. [PubMed: 18270714]
18. Jansen SA, Fan X, Karczmar GS, et al. Differentiation between benign and malignant breast lesions detected by bilateral dynamic contrast-enhanced MRI: a sensitivity and specificity study. Magn Reson Med. 2008; 59(4):747–54. [PubMed: 18383287]
19. Dixon WT. Simple proton spectroscopic imaging. Radiology. 1984; 153(1):189–94. [PubMed: 6089263]
20. Pruessmann KP, Weiger M, Scheidegger MB, Boesiger P. SENSE: sensitivity encoding for fast MRI. Magn Reson Med. 1999; 42(5):952–62. [PubMed: 10542355]
21. Griswold MA, Jakob PM, Heidemann RM, et al. Generalized autocalibrating partially parallel acquisitions (GRAPPA). Magn Reson Med. 2002; 47(6):1202–10. [PubMed: 12111967]
22. Friedman P, Swaminathan S, Smith R. SENSE imaging of the breast. AJR Am J Roentgenol. 2005; 184:448–51. [PubMed: 15671362]
23. Ramsay E, Causer P, Hill K, Plewes D. Adaptive bilateral breast MRI using projection reconstruction time-resolved imaging of contrast kinetics. J Magn Reson Imaging. 2006; 24:617–24. [PubMed: 16892204]
24. Dougherty L, Isaac G, Rosen MA, et al. High frame-rate simultaneous bilateral breast DCE-MRI. Magn Reson Med. 2007; 57(1):220–5. [PubMed: 17152087]
25. Herrmann KH, Baltzer PA, Dietzel M, et al. Resolving arterial phase and temporal enhancement characteristics in DCE MRM at high spatial resolution with TWIST acquisition. J Magn Reson Imaging. 2011; 34(4):973–82. [PubMed: 21769981]
26. Saranathan M, Rettmann DW, Hargreaves BA, et al. DIfferential subsampling with Cartesian ordering (DISCO): a high spatio-temporal resolution Dixon imaging sequence for multiphasic contrast enhanced abdominal imaging. J Magn Reson Imaging. 2012; 35(6):1484–92. [PubMed: 22334505]
27. Song T, Laine AF, Chen Q, et al. Optimal k-space sampling for dynamic contrast-enhanced MRI with an application to MR renography. Magn Reson Med. 2009; 61(5):1242–8. [PubMed: 19230014]
28. Le Y, Kipfer H, Majidi S, et al. Application of time-resolved angiography with stochastic trajectories (TWIST)-Dixon in dynamic contrast-enhanced (DCE) breast MRI. J Magn Reson Imaging. 2013; 38(5):1033–42. [PubMed: 24038452]

29. Saranathan M, Rettmann DW, Hargreaves BA, et al. Variable spatiotemporal resolution three-dimensional Dixon sequence for rapid dynamic contrast-enhanced breast MRI. J Magn Reson Imaging. 2014; 40(6):1392–9. [PubMed: 24227703]
30. Mostardi PM, Haider CR, Rossman PJ, et al. Controlled experimental study depicting moving objects in view-shared time-resolved 3D MRA. Magn Reson Med. 2009; 62(1):85–95. [PubMed: 19319897]
31. Johnson CP, Polley TW, Glockner JF, et al. Buildup of image quality in view-shared time-resolved 3D CE-MRA. Magn Reson Med. 2013; 70(2):348–57. [PubMed: 22936574]
32. Ma J. Breath-hold water and fat imaging using a dual-echo two-point Dixon technique with an efficient and robust phase-correction algorithm. Magn Reson Med. 2004; 52(2):415–9. [PubMed: 15282827]
33. Le-Petross H, Kundra V, Szklaruk J, et al. Fast three-dimensional dual echo dixon technique improves fat suppression in breast MRI. J Magn Reson Imaging. 2010; 31(4):889–94. [PubMed: 20373433]
34. van Vaals JJ, Brummer ME, Dixon WT, et al. “Keyhole” method for accelerating imaging of contrast agent uptake. J Magn Reson Imaging. 1993; 3(4):671–5. [PubMed: 8347963]
35. Mann R, Mus R, van Zelst J, et al. A novel approach to contrast-enhanced breast magnetic resonance imaging for screening: High-resolution ultrafast dynamic imaging. Investigative Radiol. 2014; 49(9):579–85.
36. Tudorica LA, Oh KY, Roy N, et al. A feasible high spatiotemporal resolution breast DCE-MRI protocol for clinical settings. Magn Reson Imaging. 2012; 30(9):1257–67. [PubMed: 22770687]
37. Henderson E, Rutt B, Lee T. Temporal sampling requirements for the tracer kinetics modeling of breast disease. Magn Reson Imaging. 1998; 16(9):1057–73. [PubMed: 9839990]
38. Yankeelov TE, Gore JC. Dynamic Contrast Enhanced Magnetic Resonance Imaging in Oncology: Theory, Data Acquisition, Analysis, and Examples. Curr Med Imaging Rev. 2009; 3(2):91–107. [PubMed: 19829742]
39. DCE-MRI Technical Committee. Quantitative Imaging Biomarkers Alliance. Version 1.0. Publicly Reviewed Version. QIBA; Jul 1. 2012 DCE-MRI Quantification Profile. Available from: RSNA.org/QIBA
40. Huang W, Li X, Chen Y, et al. Variations of Dynamic Contrast-Enhanced Magnetic Resonance Imaging in Evaluation of Breast Cancer Therapy Response: A Multicenter Data Analysis Challenge. Translational Oncology. 2014; 7(1):153–66. [PubMed: 24772219]
41. Kuhl CK, Schrading S, Strobel K, et al. Abbreviated Breast Magnetic Resonance Imaging (MRI): First Postcontrast Subtracted Images and Maximum-Intensity Projection-A Novel Approach to Breast Cancer Screening With MRI. J Clin Oncol. 2014; 32(22):2304–10. [PubMed: 24958821]
42. Holmes, JH., Wang, K., Morrison, CK., et al. Mitigating bias and variance associated with fat signal in quantitative DCE of the breast. Proceedings of the Annual Meeting of ISMRM; Toronto. 2015. abstract 0191
43. Le Y, Dale B, Akisik F, et al. Improved T1, contrast concentration, and pharmacokinetic parameter quantification in the presence of fat with two-point Dixon for dynamic contrast-enhanced magnetic resonance imaging. Magn Reson Med. 2016; 75(4):1677–84. [PubMed: 25988338]

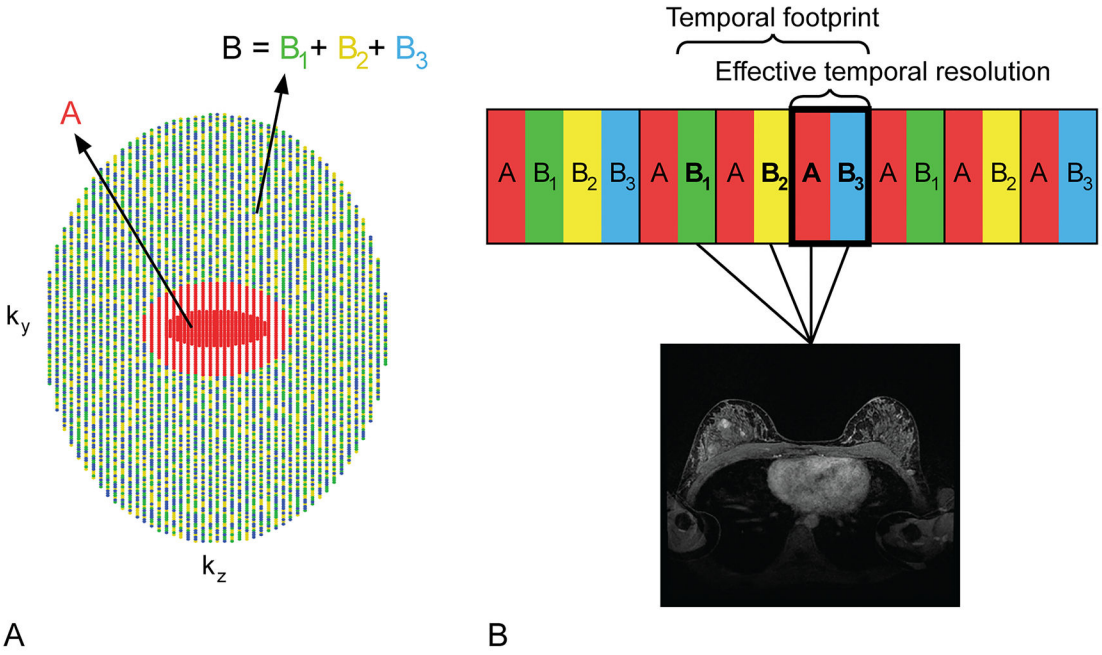

Figure 1.

(A) High spatiotemporal resolution T_1-weighted DCE MRI was achieved using variable density, pseudo-random k-space sampling with a fully-sampled central “A” region, which consisted of 16% of the k-space views and was acquired in each k-space interval (red region), and a peripheral “B” region, one-third of which was acquired in each k-space interval (green, yellow, and blue regions). (B) Images for a single time frame were produced using data from a full k-space interval and the appropriate B sub-region data from the two preceding k-space intervals in order to create a fully-sampled k-space volume (backward view sharing). For example, images for a single, fully-sampled time frame (dark box) would be reconstructed using the A region and B sub-region acquired during one k-space interval (red and blue boxes within the dark box with lines leading to the MR image) and two B sub-regions from preceding k-space intervals (yellow and green boxes with lines leading to the MR image). The time required to collect all the data used for reconstruction of a single, fully-sampled time frame, including the data shared from neighboring k-space intervals, is called the temporal footprint, while the effective temporal resolution refers to the time between the acquisitions of the central region of k-space.

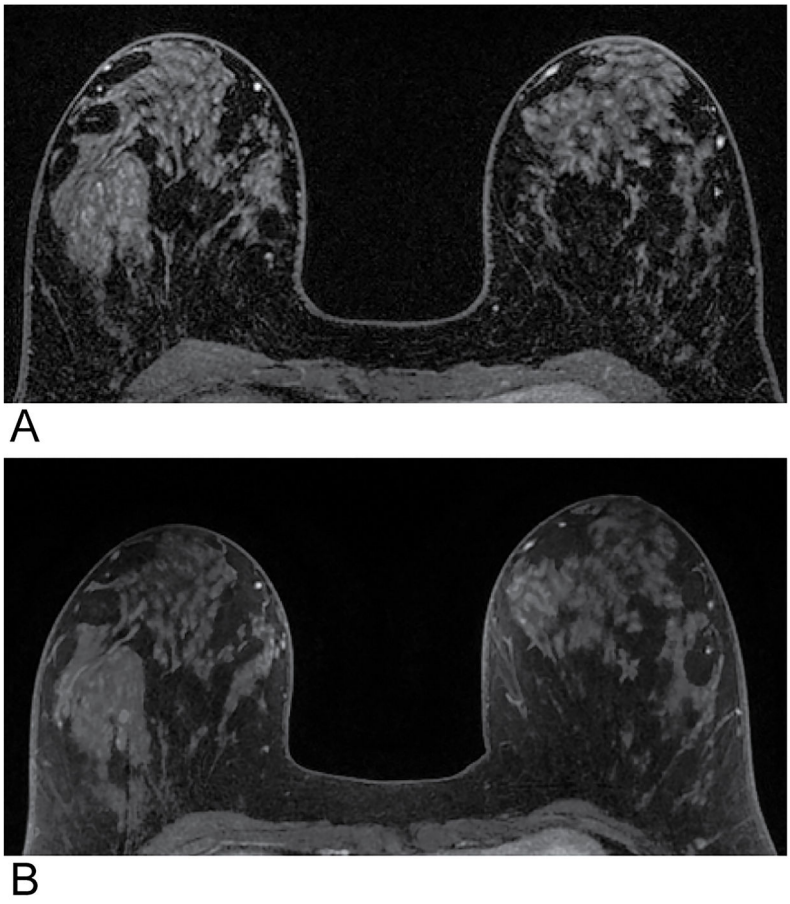

Figure 2.

Magnified and cropped T1-weighted axial images of a single slice from a post-contrast time frame from a single patient demonstrating the improved fat suppression obtained using DISCO (A) compared with the standard-of-care method (B). The mean scores for the fat suppression of DISCO and the standard-of-care method were 9.0 and 8.3, respectively.

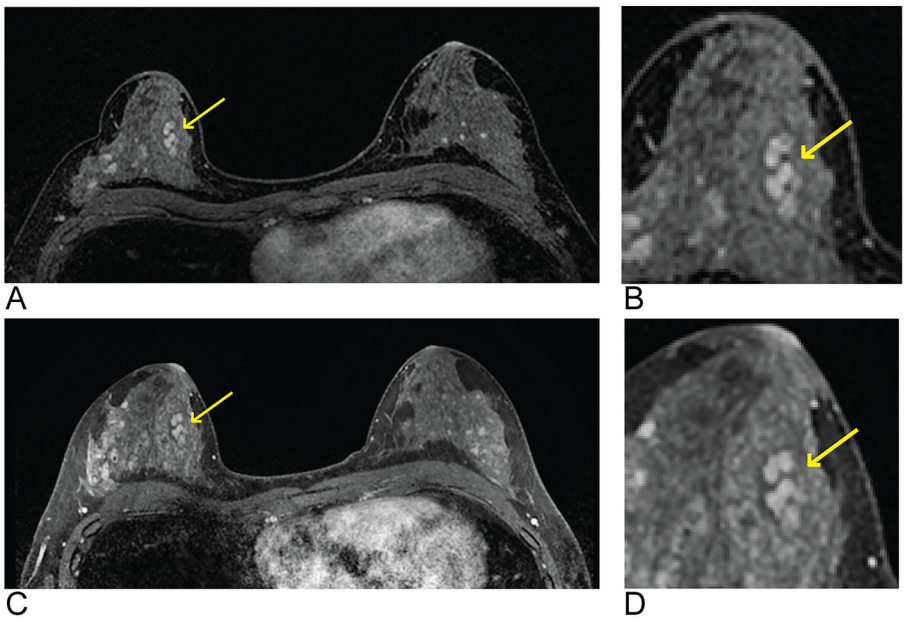

Figure 3.

Representative images of a single axial slice from a T1-weighted post-contrast time frame from a single patient demonstrating the comparable image quality obtained using DISCO (A and B) and the standard-of-care method (C and D). The lesion (arrows) is a biopsy-proven benign fibroadenoma with dark internal septation well-depicted with both methods. A magnified and cropped region with the lesion of interest is shown for both DISCO (B) and the standard-of-care method (D). The mean overall image quality scores were both as 8.0 for DISCO and the standard-of-care method, and lesion conspicuity was scored as 8.7 and 7.7, respectively.

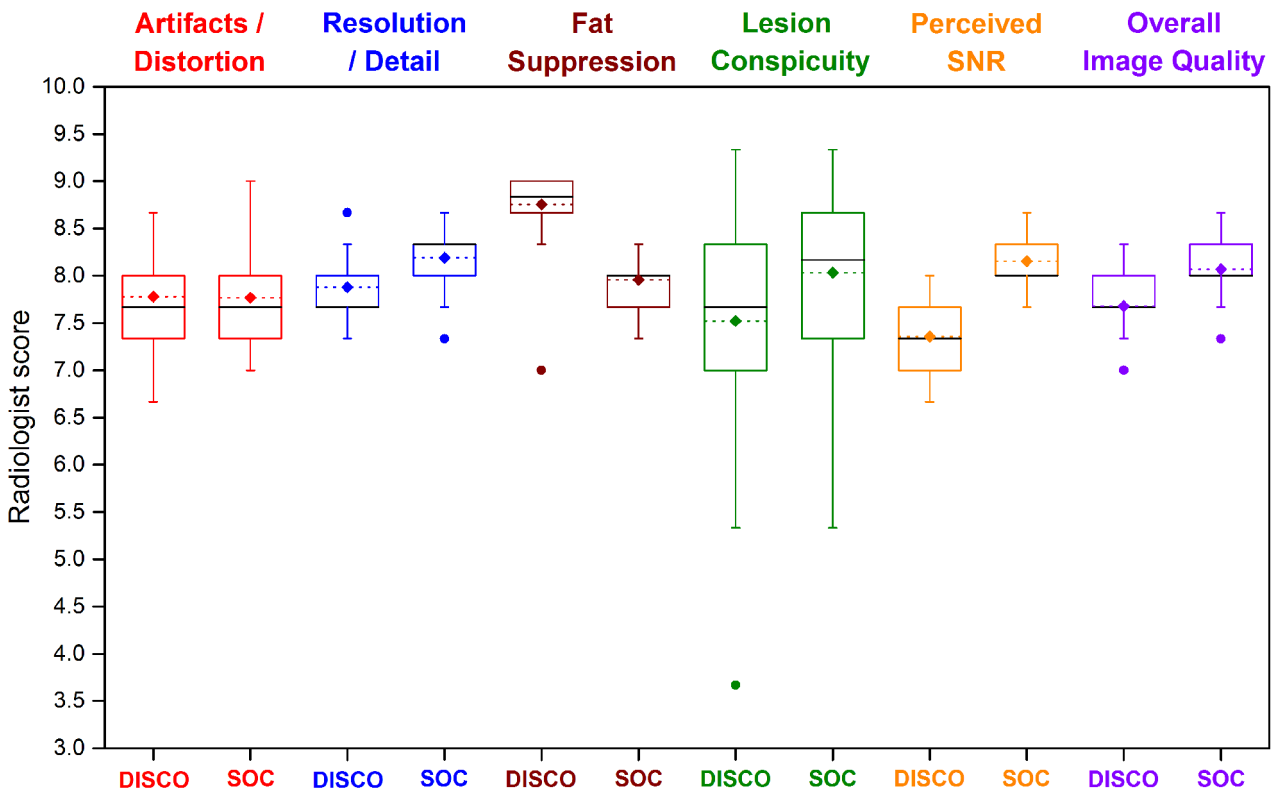

Figure 4.

Boxplot of the mean reader scores per patient for all image quality categories. Median (black lines), mean (dotted lines with diamonds), and outliers (dots) are indicated. Whiskers represent 1.5 times the interquartile range. Images were scored as 6 or higher for both DISCO and the standard-of-care method in all categories with the exception of three cases for the DISCO method and one case for the standard-of-care method which all scored below 6 for lesion conspicuity.

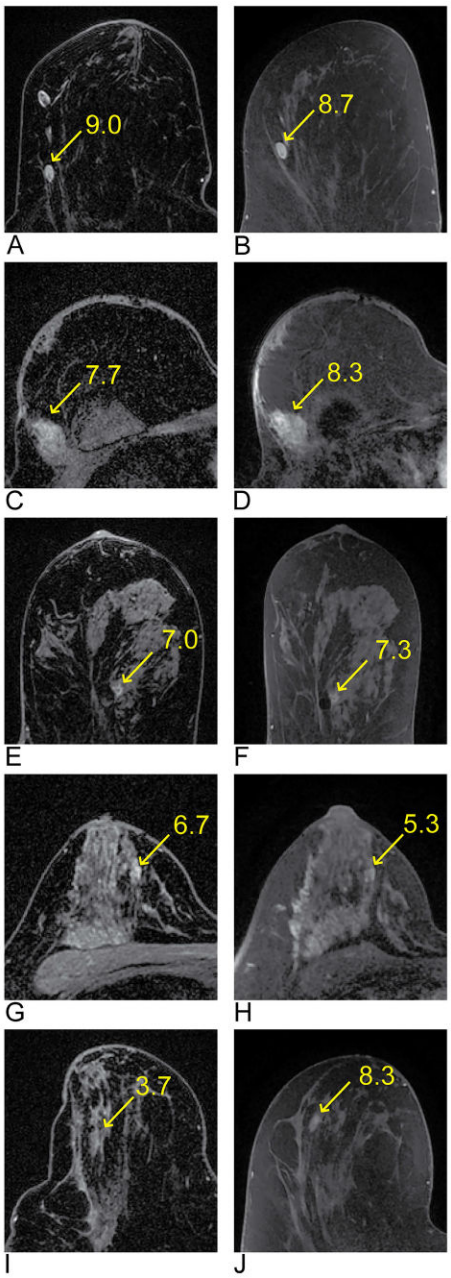

Figure 5.

Examples of lesions that were included in the image quality assessment and demonstrate a range of lesion conspicuity scores. DISCO images are on the left and the SOC images are on the right. The images show the following lesions indicated by the arrows: lymph node (A and B), fat necrosis (C and D), fibrocystic changes (E and F), focal area of benign background parenchymal enhancement (G and H), and a lesion that is benign with two years follow-up (I and J). The corresponding lesion conspicuity score is next to the arrow on each image.

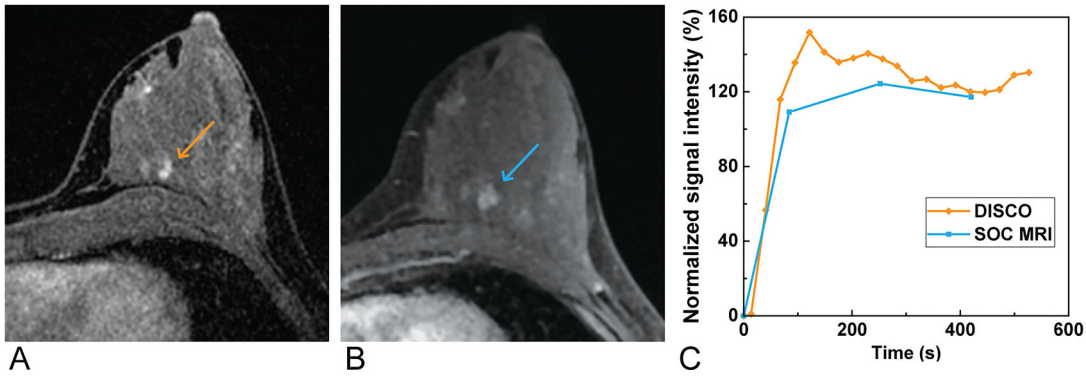

Figure 6.

Magnified and cropped region from an axial slice from a T1-weighted post-contrast time frame from a single patient obtained using DISCO (A) and the standard-of-care method (B) demonstrating preserved image quality with DISCO. A plot of the signal intensity-time curve (C) from an ROI placed in one of the lesions in the left breast (arrows) demonstrates multiple additional time points given the better effective temporal resolution, and thus greater signal intensity-time curve detail, obtained using DISCO (orange curve) compared with the standard-of-care method (SOC method, blue curve).

Table 1

Breast MRI acquisition parameters

Parameter	DISCO	Standard-of-care MRI
Fat suppression	2-point Dixon	Intermittent fat saturation
Repetition time (ms)	7.8	6.0
First / second echo time (ms)	2.2 / 4.6	2.9
Flip angle (°)	10	10
Field of view (mm^2)	340 × 340	320 × 320
Matrix size	412 × 412	384 × 384
Slice thickness (mm)	1.6	1.6
Voxel volume (mm^3)	0.8 × 0.8 × 1.6	0.8 × 0.8 × 1.6
Receiver bandwidth (kHz)	± 83.3	± 50.0
Parallel imaging method	ARC	ASSET
Parallel imaging factors ($k_z \times k_y$)	2 × 2	2 × 1
Effective temporal resolution (s)	27	168

Table 2

Pooled mean reader scores for three readers by image quality category (1=worst, 10=best)

Category	DISCO	Difference (standard error)	Standard-of-care MRI
Image distortion / artifacts	7.8	= 0.0 (0.1) p = 0.91	7.8
Resolution / detail	7.9	→ 0.3 (0.07) p < 0.01	8.2
Fat suppression	8.8	← 0.8 (0.08) p < 0.01	8.0
Lesion conspicuity	7.5	→ 0.5 (0.21) p = 0.02	8.0
Perceived SNR	7.4	→ 0.8 (0.07) p < 0.01	8.2
Overall image quality	7.7	→ 0.4 (0.07) p < 0.01	8.1